Colloids and Surfaces B: Biointerfaces 111 (2013) 354–359

Contents lists available at SciVerse ScienceDirect

Colloids and Surfaces B: Biointerfaces

journal homepage: www.elsevier.com/locate/colsurfb

Real-time study of protein adsorption kinetics in porous silicon

Liliana C. Lasave[a,*], Raúl Urteaga[a,b], Roberto R. Koropecki[a,b], Verónica D. Gonzalez[a], Roberto D. Arce[a]

[a] INTEC (UNL-CONICET), Güemes 3450, 3000 Santa Fe, Argentina
[b] Facultad de Ingeniería Química (UNL), Santiago del Estero 2829, 3000 Santa Fe, Argentina

ARTICLE INFO

Article history:
Received 6 December 2012
Received in revised form 11 May 2013
Accepted 5 June 2013
Available online xxx

Keywords:
Protein adsorption
Kinetics
Porous silicon

ABSTRACT

This paper presents an optical method for real-time monitoring of protein adsorption using porous silicon self-supported microcavities as a label-free detection platform. The study combines an experimental approach with a physical model for the adsorption process. The proposed model agrees well with experimental observations, and provides information about the kinetics of diffusion and adsorption of proteins within the pores, which will be useful for future experimental designs.

1. Introduction

The phenomenon of protein adsorption to solid surfaces plays an important role in many disciplines, such as biomedical sciences or biochemical engineering. In order to achieve optimal performance of certain materials and processes, it is crucial to control and manipulate the interaction between surfaces and proteins [1,2]. However, to reach that level of understanding, it is essential to have knowledge about the kinetics of the events occurring during each specific situation. Common techniques to study the kinetics by which a surface is covered with proteins are: surface plasmon resonance, ellipsometry, fluorescence detection, Fourier transform infrared (FTIR) spectroscopy, atomic force microscopy (AFM), gravimetric techniques (QCM, QCM-D, SAW-devices) and radiolabeling methods [3,4]. These measurement techniques are expensive, time-consuming, and they need highly trained operators or hazardous reagents. Therefore, the aim of this work is to develop a methodology to monitor the process in real time. This methodology should be not only simple, but also inexpensive, and label-free at the same time.

Porous silicon (PS) grown from Si wafers is a very attractive material for biomedical applications due to their remarkable optical and morphological properties. Such properties depend primarily on the substrate doping and orientation of the wafer, as well as on the electrolyte composition, and on the applied current density during the anodization process [5]. Thus, it is possible to fabricate PS with pore sizes ranging from a few nanometers to several micrometers [6]. After the etching process, it is possible to detach PS structures from the crystalline silicon substrate by applying a pulse of high current density. These free-supporting films can then be easily transferred to other media such as glass slides. This procedure facilitates measurements of some optical properties of the PS devices, avoiding the interference of the silicon wafer, which is lying at the bottom of the sample in the undetached films [7].

For sensing applications, it is necessary to modify the PS surface since the freshly etched material has some drawbacks such as hydrophobicity (due to hydrogen-terminated porous silicon groups ($S—H_x$) [8]), and lack of stability in aqueous environments [9]. It has been demonstrated that thermal oxidation can be used to impart greater stability to the PS samples in aqueous solutions, and also to create hydrophilic pore channels [10]. Structural stabilization and oxide formation have also been reported following heat treatment at 300 °C [11]. PS is a material of choice for many of these applications since its refractive index is very sensitive to the treatments experienced by its surface [12]. In particular, this parameter decreases during oxidation, due to the smaller refractive index of silicon oxide compared to crystalline silicon. When molecules with similar size to the pore diameter penetrate into the porous matrix, they produce an appreciable change in the effective refractive index of the material [13]. As a result of this property, PS has become an ideal candidate for the development of chemical and biological sensors.

The PS microcavities are Fabry–Perot resonators sandwiched by two distributed Bragg reflectors (BR). The BR is constructed by

* Corresponding author at: Instituto de Desarrollo Tecnológico para la Industria Química, UNL-CONICET, Güemes 3450, 3000 Santa Fe, Argentina.
Tel.: +54 0342 455 9174.
E-mail addresses: llasave@intec.unl.edu.ar, lilianacl@gmail.com (L.C. Lasave).

0927-7765/$ – see front matter © 2013 Elsevier B.V. All rights reserved.
http://dx.doi.org/10.1016/j.colsurfb.2013.06.024

stacking thin layers of alternating low and high porosity with a quarter wave optical thickness [14]. The optical response of the microcavity shows a high reflectivity band with one or more transmittance peaks. There are several experimental techniques to study the incorporation of molecules into PS structures: interferometric reflectance spectroscopy [15,16], photoluminescence [17], electroluminescence [18,19] and spectroscopic ellipsometry [20,21]. Most studies of protein adsorption on PS, have been carried out by using spectroscopic ellipsometry [22–24]. In this work, a near-normal incidence reflectance spectroscopy technique has been chosen for its speed, simplicity and low cost. This technique has been widely used in the investigation of several structural and optical properties of porous silicon [25]. This research analyzes the adsorption kinetics of proteins onto oxidized PS microcavities using real-time reflectance spectroscopy. This technique detects small changes in the effective refractive index of porous silicon devices through quantitative spectra shifts. These changes can correlate with the incorporation of protein in the porous matrix.

In order to analyze the results, a model that includes diffusion rate in the pore and finite adsorption kinetics is presented. Two characteristic times could be detected: one attributable to the diffusion process and the other corresponding to the adsorption process itself. These parameters are not only useful to characterize the measurement system developed, but also to optimize the sensing time and the use of reagents. The theoretical and practical system proposed in this work could be applied to study bioaffinity interactions between the biomolecules immobilized on the surface (that is, the biological receptors) with specific analytes of interest present in a sample. The application of such protein-modified devices could lead to important contributions to relevant diagnostic problems as early detection of pathogens, cancer and other diseases in real biological samples.

2. Experimental details

Porous silicon samples were prepared from highly doped (boron) p+ ⟨1 0 0⟩ silicon wafers with a resistivity of 0.002–0.004 $m\Omega\,cm^{-1}$. The preparation method used was electrochemical etching [26] at room temperature in a standard Teflon etch cell using an electrolyte solution which contained hydrofluoric acid (50%) and ethanol mixed in a ratio 1:2 (v/v).

PS microcavities centered in $\lambda_c \sim 730$ nm alternating two types of layers were fabricated and the scheme of high (H) and low (L) current density layers that was followed was: 5HL 30H 4.5LH. All layers had an optical thickness equal to $\lambda_c/4$, except the central defect which had $30\lambda_c/4$. The quality factor (Q) of the wet microcavities was in the range from 50 to 70.

The optical parameters (physical thickness and porosity) needed to design the optical microcavities were obtained by fitting the reflectance spectra of PS single layers [27]. The set of current densities chosen was 57.3 mA/cm^2 for high porosity layers (80%) and 12.7 mA/cm^2 for low porosity layers (60%).

The hydraulic radius of the pores was estimated from scanning electron microscope (SEM) photomicrographs, and turned out to be about 40 nm for 57.3 mA/cm^2 layers and 13 nm for 12.7 mA/cm^2 layers [7].

The porosity of the layers had to be chosen in order to allow the protein to enter the pores. Since the contrast of selected porosity was not very high, a long central defect was chosen to increase the quality factor of the resonance peak. A sharper peak is more sensitive to small changes in the effective refractive index of the porous matrix. After the etching process and in order to separate the porous silicon microcavities from the silicon wafer, three pulses of 250 mA/cm^2 were applied using an etching solution of hydrofluoric acid and ethanol, mixed in a ratio 1:7 (v/v). Each self-supporting sample was rinsed with ethanol and divided into 4 parts. Then, each piece of sample was transferred to a glass slide and dried under a stream of N_2 gas. All samples were thermally oxidized. Dry thermal oxidation was conducted in air atmosphere at 300 °C for 120 min. For each series of measurements different parts of the same microcavity were taken to minimize the errors due to the variability of different samples.

Both single layers and multilayers were characterized by reflectance spectroscopy in the visible to near-infrared region by using an Ocean Optics fiber optic spectrometer HR4000. The porosity values of the PS single layers were estimated from the reflectance spectra in the range of 200–1100 nm [7,27].

In this paper, glucose oxidase and horseradish peroxidase were employed as model proteins for being well-characterized and robust molecules as well as for their different molecular size. As mentioned above, when working with biological macromolecules, the molecular size is a critical parameter for the incorporation of such molecules into the porous matrix. The glucose oxidase enzyme (GOx) is a globular glycoprotein containing approximately 16% neutral sugar and 2% of amino sugars. It has an overall dimension of 6.0 nm × 5.2 nm × 7.7 nm [28], a molecular weight of 160 kDa, and it is a dimer of two identical subunits. Its hydrodynamic radius is equal to 4.3 nm [29] and its isoelectric point is equal to 4.2 [30]. On the other hand, horseradish peroxidase enzyme (HRP) is also a glycoprotein but in this case it contains 18% carbohydrate. It has a molecular weight of 44 kDa, an isoelectric point of 7.2 and a hydrodynamic radius equal to 2.5 nm [31]. Different amounts of each protein were dissolved in 2 mM sodium acetate buffer, pH 5, to obtain protein solutions between 0.25 and 3.00 mg/mL.

2.1. Measurement system

Fig. 1 shows the system employed to measure light reflection from self-supporting PS microcavities during the protein adsorption process. The same optical fiber was used to illuminate the sample with white light source and to collect the reflected light over time. Reflectivity data were recorded in a CCD detector (Ocean Optics spectrometer HR4000) in the wavelength range of 200–1100 nm. As the scheme shows, the process takes place in a closed compartment and data are acquired illuminating the sample through the glass slide. This configuration is advantageous when working with hazardous samples.

A spectral acquisition time of 1 s and a typical average of 4 spectral scans (4 s total integration time) were selected. After each set of scans, a Gaussian fit of the resonant microcavity central peak was performed to monitor its position as a function of time.

The procedure performed in all the experiments was as follows: (1) pumping a solution of 70% of ethanol to clean the PS surface and render it hydrophilic, (2) pumping acetate buffer to rinse and prepare the PS surface, and (3) pumping the protein solution into the flow cell at a flow rate of 50 μL/s using a peristaltic pump for 30 s and then the output of the cell was closed to prevent further movement of the liquid. Each adsorption was performed in different pieces of the same microcavity and all the experiments were carried out at a constant temperature.

2.2. Theoretical model

As we have shown in a previous paper, the PS spectrum of the microcavity is altered only when the solution which penetrates the porous structure reaches the region of the defect. In order to reach the defect, the protein must diffuse through the frontal Bragg mirror. This means that the protein solution suffers a diffusion process through a porous media. Assuming that the pore

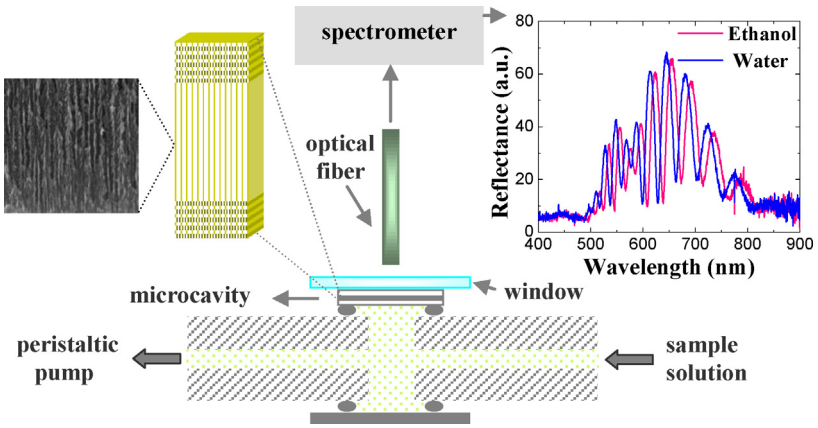

Fig. 1. Scheme showing the set up used to measure protein adsorption onto PS self-supporting microcavities. The total volume of the cell is 50 μL. The figure also shows a 400 nm side SEM photomicrograph corresponding to the microcavity defect. In the upper part of the figure it is shown the spectral shift which occurs when the device is immersed in water or ethanol.

structure is predominantly unidimensional, the protein flux J_D can be calculated by the Fick's law [32] as:

$$J_D = D_{eff}\frac{\partial c}{\partial x}$$

where c is the protein concentration, t is the time, and x the length. Here D_{eff} is an effective diffusion constant defined as [33]:

$$D_{eff} = \frac{D\varepsilon\delta}{\tau}$$

where D is the diffusion constant of the protein in the buffer, τ the tortuosity, δ the constriction factor, and ε the porosity. The dimensionless constants τ, δ and ε depend on the particular porous structure under consideration.

In order to model our data, we propose a simplified model for the diffusion through the Bragg mirror. The simplification consists of replacing the concentration gradient by the ratio $\Delta c/\Delta x$. In this way we assume that the flux of protein entering the defect (J_D) is directly proportional to the difference between the protein concentration in the solution outside the microcavity (c_{max}) and the concentration of unbound protein in the solution inside the defect region at a given time (c_U). This can be express as follows:

$$J_D \cong D_{eff}\frac{c_{max} - c_U}{\Delta x} \quad (1)$$

where Δx is the width of the frontal Bragg mirror. The central defect width of the cavity may be disregarded in comparison of the Bragg mirror width, and the protein concentration in this region c_U can be assumed as a constant that depends only on time. A schematic diagram of the process is shown in Fig. 2.

The evolution of the protein concentration within the defect (c_T) volume will be:

$$\frac{\partial c_T}{\partial t} = \frac{JA}{V} = \frac{JA}{Ad} = \frac{J}{d} \quad (2)$$

In this expression A, V and d corresponds to the transversal area, the volume and the length of the defect respectively. Once the proteins are inside the cavity, the process of adsorption occurs. The concentration c_T represents the total protein concentration composed by an unbound part c_U and a bound portion c_B attached to the pore walls in the defect. Combining Eqs. (1) and (2), we have

$$\frac{\partial c_T}{\partial t} = \frac{D_{eff}}{\Delta x.d}(c_{max} - c_U) = k_{diff}(c_{max} - c_U) \quad (3)$$

where the inverse of k_{diff} represents a characteristic diffusion time (t_{diff}) of the protein through the porous structure.

Now consider what happens to the protein that enters the defect. Part of it will be adsorbed and part will remain in solution, changing the protein concentration in the solution. The change in the total protein concentration will produce a change in the refractive index of the cavity pores. According to reference [34] the dependence of the refractive index with the protein concentration may be expressed as:

$$\Delta n = n_{ps} - n_s = \alpha c \quad (4)$$

where n_{ps} is the refractive index of the protein solution, n_s is the refractive index of the buffer solution, c is the concentration of

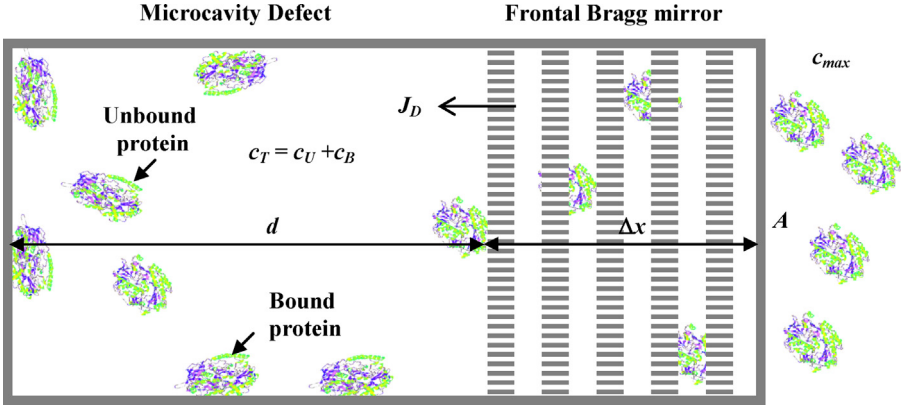

Fig. 2. Scheme of the proposed model for protein adsorption onto PS. The protein content in the porous matrix is determined by the balance between a flux of protein filling the pores and a flux of adsorption on the pore walls.

protein in the solution, and α is the proportionality constant. The reported value of α was around 0.002 (for c expressed as g/100 cc) for a broad range of proteins. Although it is not reported the value of α for GOx, we considered this as an indicative value.

If the adsorption process is reversible, replacing the solution by the corresponding buffer should produce desorption of the protein molecules. However, in general, when a protein solution in contact with a solid phase is suddenly replaced by a buffer solution, only a small fraction of the adsorbed molecules are desorbed. This is indicative of the irreversibility of the adsorption process. We performed the experiments in order to check this point in our system. For this purpose, as the saturation in the refractive index has been reached during the adsorption process, the protein solution was replaced by the corresponding buffer. As the buffer solution enters the optical cavity, we recorded a relative variation in the refractive index in the order of about 3×10^{-4}. This number is in agreement with the value expected considering that the GOx solution (1 mg/mL) has been replaced by the buffer, without producing desorption of the bound protein (Eq. (4)). In other words, it means that the adsorption process may be assumed to be irreversible.

The kinetics of the irreversible adsorption process, taking place inside the microcavity, is represented by [35]

$$\frac{\partial \Gamma}{\partial t} = k_{ad} c_U (\Gamma_{max} - \Gamma) \quad (5)$$

where Γ represents the number of active sites covered by protein molecules per unit area. Γ_{max} is the maximum number of active sites available and k_{ad} is the adsorption constant. We assume that each active site adsorbs only one molecule. Multiplying the volumetric specific surface area S_V of the microcavity defect by Γ yields the number of bound protein per unit volume, c_B. Then Eq. (5) may be written as:

$$\frac{\partial c_B}{\partial t} = k_{ad} c_U (c_{Bmax} - c_B) \quad (6)$$

The initial conditions are $c_U = 0$ and $c_B = 0$, and the total amount of protein reached in stationary conditions is $c_{Tmax} = c_{Bmax} + c_{max}$. In order to perform the fitting on the measured values is convenient to express the concentration of protein in a non-dimensional way. We use the value of c_{Tmax} to obtain the non-dimensional values for all concentration.

$$c^* = \frac{c}{c_{max} + c_{Bmax}} = \frac{c}{c_{Tmax}}$$

The change in the refractive index produced by the protein in solution (Eq. (4)) can be used to obtain the peak shift of the system trough his sensitivity ($S = \Delta\lambda/\Delta n$). In this way we can calculate the instantaneous peak shift as $\Delta\lambda = S\Delta n = S\alpha c_T$ and in stationary conditions $\Delta\lambda_{max} = S\alpha c_{Tmax}$. Taking the ratio between these expressions we obtain

$$\frac{\Delta\lambda}{\Delta\lambda_{max}} = \frac{c_T}{c_{Tmax}} = c_T^* \quad (7)$$

Thus, the normalized peak shift $\Delta\lambda/\Delta\lambda_{max}$ can be used to estimate the also normalized total concentration of proteins in the system.

The total change of unbound and bound proteins can be calculated respectively as:

$$\frac{\partial c_U^*}{\partial t} = \frac{\partial c_T^*}{\partial t} - \frac{\partial c_B^*}{\partial t} = k_{diff}(c_{max}^* - c_U^*) - k_{ad} c_U^* (1 - c_{max}^* - c_B^*)$$

$$\frac{\partial c_B^*}{\partial t} = k_{ad} c_U^* (1 - c_{max}^* - c_B^*)$$

The equation system was solved numerically using an adaptive Runge–Kutta scheme. Experimental data were fitted by minimizing the mean square error using a Nelder–Mead simplex method. In this method, the fitting parameters (k_{ad}, k_{diff} and c_{Bmax}^*) are iteratively modified in order to optimize a merit function (the mean square error in this case). Furthermore, we explore a wide region in the space of parameters and check that the merit function is smooth and have only one global minimum. In order to estimate the confidence limits on the model parameters we use Monte Carlo simulation of synthetic data sets [36].

3. Results and discussion

3.1. Device detection sensitivity

The wavelength shift sensitivity of the device was measured by liquid infiltration, evaluating the spectral shift of the microcavity ($\Delta\lambda$) by replacing the air in the pores with serial dilutions of ethanol in water. The peak shift ($\Delta\lambda$) was measured as a function of the refractive index change of the solutions Δn. The sensitivity of a measurement system is given by the slope of the calibration curve. In this case, the slope represents the wavelength shift sensitivity of the porous silicon device and its value was found to be $\Delta\lambda/\Delta n \sim 350$ nm for a peak centered in 700 nm (numerical simulation predicts $\Delta\lambda/\Delta n = 320$ nm) [37]. The minimum detectable peak shift was 5×10^{-3} nm. This means a detection limit of refractive index change of 1.4×10^{-5} that is comparable to the obtained in other experimental setups [38,39].

Fig. 3a and b shows the normalized peak shift during adsorption of glucose oxidase (the total shift was about 1.4 nm) and horseradish peroxidase (the total shift was about 1.3 nm) respectively. In both figures, the triangles correspond to the experimental data and the different curves represent the model: the dash-dotted line is the contribution of protein molecules in solution (c_U^*), the dashed line is the contribution of protein adsorbed (c_B^*), and the black curve (the result from fitting the experimental points using the proposed model) is the total protein content (c_{Tmax}^*). The three fitted parameters are shown in the figures.

As expected, the diffusion time (t_{diff}) is longer for the largest protein. The diffusion time of GOx was almost 4 times longer than the diffusion time of HRP. The diffusion coefficients here reported cannot be used to compare directly with those obtained in another experimental setup. This is because this parameter depends not only on the nature of the molecule but also on the characteristics of the porous matrix used.

The adsorption constant (k_{ad}) is smaller for HRP than for GOx by a factor of 6. We cannot compare directly these values, since the proteins used were different in sequence, size and net charge.

Nevertheless, k_{ad} can be a useful parameter to compare the same protein in different conditions as pH, temperature, or in a variety of porous matrix characteristics. It has been reported that the initial adsorption rate is higher at a pH near the isoelectric point of the protein than for other pH, which indicates a strong correlation between the adsorption kinetics and the protein charge [40]. These observations are consistent with the higher adsorption velocity of glucose oxidase in the experiments taking into account the isoelectric point of each protein, and the experimental conditions, GOx molecules have a net charge close to zero, while HRP molecules are positively charged at pH 5.

Fig. 4 shows the maximum peak shift resulting from the adsorption of GOx at 24 °C for different protein concentrations (adsorption isotherm). The total peak shift (squares) corresponds to the contribution of both: the protein in solution (circles) and the adsorbed protein (triangles).

Although the resonance peak shift always increases with protein concentration, the adsorbed protein (c_B) calculated from the fit saturates at concentrations of 1.00 mg/mL. For higher concentrations, the peak shift rises only with the increase of protein content in the

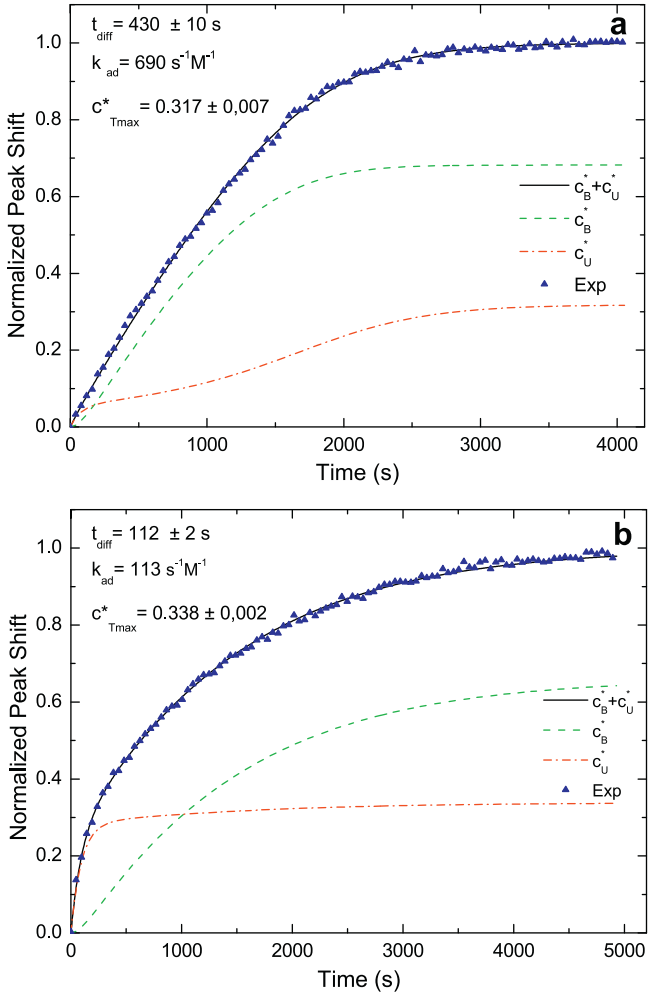

Fig. 3. (a) Normalized resonance shift during adsorption of 1 mg/mL GOx at 25.5 °C, 2 mM sodium acetate buffer, at pH 5 (triangles). The curves represent the adsorption model as explained in the text. (b) Normalized resonance shift during adsorption of 0.3 mg/mL HRP at 24.2 °C, 2 mM sodium acetate buffer, at pH 5 (triangles). The curves represent the adsorption model as explained in the text.

solution (c_U). This indicates that 1.00 mg/mL is the concentration that produces saturation of all available binding sites on the surface. It is worth noticing that the adsorbed protein on the surface at 1.00 mg/mL is 5 times larger than the free protein in the solution.

According to the literature, the specific surface area (SSA) of a porous matrix similar to the one that forms the defect of the microcavities (measured by nitrogen adsorption isotherms using the Brunauer–Emmett–Teller (BET) method), is in the range of 150 to 200 m^2/cm^3 [41]. The estimated SSA of the samples from SEM photomicrographs (Fig. 1) is found to be about 110 m^2/cm^3. The area per GOx molecule depends on the morphology of the adsorbed molecule but can be estimated as approximately 58 nm^2 [42].

Considering that the material studied has a distribution of pore dimensions (see Fig. 1) and that nitrogen molecules are smaller than protein molecules, the first would have access to a wider range of pore sizes than the second ones. In such a case, the SSA value obtained by BET overestimates the SSA which is actually available for protein adsorption.

The protein surface coverage can be evaluated considering the relationship between the free and adsorbed molecules to be proportional to the relative peak shift (c^*_{Umax}/c^*_{Bmax}). Then, the number of adsorbed proteins per unit volume can be calculated from the free molecules in the voids of the microcavity, in accordance with the solution concentration.

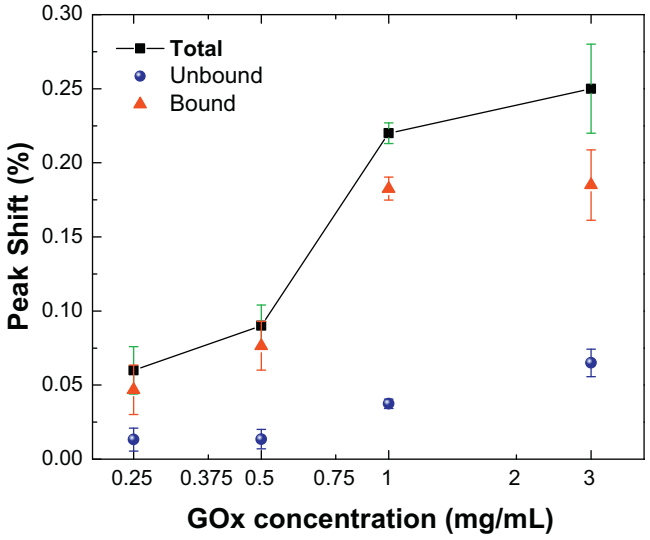

Fig. 4. Relative shift of the microcavity peak at long times (saturation) for different concentrations of GOx in a 2 mM sodium acetate buffer (pH 5), at 24.0 °C (squares). It is also shown the decomposition in free (circles) and adsorbed (triangles) portions obtained from the model fitting. The error bars come from the experimental uncertainty of the total peak shift, in all cases, to which is added the error due to the fitting process, in the case of the circles and triangles.

Considering these values, the level of PS surface coating turned out to be about 1% of the total surface. This result suggests that a high proportion of the surface is inaccessible due to size constraints. Increasing the pore diameter, a higher coverage can be attained which will improve the response. Conversely, in the case of larger pores, some drawbacks could be expected such as decreases in the specific area as well as in the response and in the quality of the microcavity. Therefore, to maximize the response for each protein, it is necessary to find the minimum value of pore size that allows an optimal surface coverage.

4. Conclusions

Spectrometric measurements in the visible range using self-sustaining porous silicon microcavities have proved to be a suitable methodology for label-free detection of protein adsorption, in real time. The resolution of the measurement system in terms of refractive index change, was about one part in 10^5.

The proposed model allows to estimate key kinetic parameters associated with the physical adsorption of proteins on porous silicon surfaces. Analyzing the kinetics parameters associated with the processes, it will be possible to make predictions of the phenomenon which will be useful for future experimental designs. This model analyzes the process of diffusion and adsorption occurring on the surface of oxidized PS in contact with a protein solution providing information about the kinetics of the adsorption, in particular, the relation between the free and adsorbed protein and the characteristic time of each process. The adsorption of GOx is limited by the protein diffusion velocity whereas the HRP is limited by the adsorption velocity itself. It was found that the amount of adsorbed molecules remains almost constant for GOx concentrations beyond 1 mg/mL. These results indicate that the saturation of the available binding sites in the pores has been reached.

Acknowledgements

We would like to thank Ramón Saavedra, for his technical support. This work was funded by grants from ANPCYT (PICT 2010 bicentenario 0135) and from Universidad Nacional del Litoral (project CAID 2009 no 68-343).

References

[1] J. Gray, Curr. Opin. Struct. Biol. 14 (2004) 110.
[2] M. Wahlgren, T. Arnebrant, Trends Biotechnol. 9 (1991) 201.
[3] P. Roach, D. Farrar, C.C. Perry, J. Am. Chem. Soc. 127 (2005) 8168.
[4] B. Kasemo, Surf. Sci. 500 (2002) 656.
[5] A. Jane, R. Dronov, A. Hodges, N.H. Voelcker, Trends Biotechnol. 27 (2009) 230.
[6] S.M. Weiss, P.M. Fauchet, IEEE J. Quantum Electron. 12 (2006) 1514.
[7] L.N. Acquaroli, R. Urteaga, C.L.A. Berli, R.R. Koropecki, Langmuir 27 (2011) 2067.
[8] O. Bisi, S. Ossicini, L. Pavesi, Surf. Sci. Rep. 38 (2000) 1.
[9] G. Palestino, R. Leprosa, V. Agarwal, E. Pérez, C. Gergely, Sens. Actuators B 135 (2008) 27.
[10] L.A. DeLouise, B.L. Miller, Anal. Chem. 76 (2004) 6915.
[11] R.B. Bjorklund, S. Zangooie, H. Arwin, Langmuir 13 (1997) 1440.
[12] M. Sailor, ACS Nano 1 (2007) 248.
[13] G. Rong, S.M. Weiss, Proc. S.P.I.E.-Int. Soc. Opt. Eng. 6769 (2007) 6769091.
[14] L. Pavesi, Nuovo Cimento Soc. Ital. Fis. 20 (1997) 1.
[15] V.S.-Y. Lin, K. Motesharei, K.-P.S. Dancil, M.J. Sailor, M.R. Ghadiri, Science 278 (1997) 840.
[16] E.J. Szili, A. Jane, S.P. Low, M. Sweetman, P. Macardle, S. Kumar, R.S.C. Smart, N.H. Voelcker, Sens. Actuators B 160 (2011) 341.
[17] S. Chan, S.R. Horner, P.M. Fauchet, B.L. Miller, J. Am. Chem. Soc. 123 (2001) 11797.
[18] V. Lehmann, Electrochemistry of Silicon: Instrumentation, Science, Materials and Applications, Wiley-VCH Verlag GmbH, Weinheim, 2002 (Chapter 10).
[19] A. Tsargorodskaya, A.V. Nabok, A.K. Ray, IEE Proc. Circ. Dev. Syst. 150 (2003) 355.
[20] S. Zangooie, R. Bjorklund, H. Arwin, Sens. Actuators B 43 (1997) 168.
[21] H. Arwin, M. Gavutis, J. Gustafsson, M. Schultzberg, S. Zangooie, P. Tengvall, Phys. Stat. Sol. A 182 (2000) 515.
[22] S. Zangooie, R. Bjorklund, H. Arwin, Thin Solid Films 313 (1998) 825.
[23] L.M. Karlsson, M. Schubert, N. Ashkenov, H. Arwin, Thin Solid Films 455 (2004) 726.
[24] L.M. Karlsson, M. Schubert, N. Ashkenov, H. Arwin, Phys. Stat. Sol. C 2 (2005) 3293.
[25] W. Theiß, Surf. Sci. Rep. 29 (1997) 91.
[26] L.N. Acquaroli, R. Urteaga, R.R. Koropecki, Sens. Actuators B 149 (2010) 189.
[27] G. Priano, L.N. Acquaroli, L.C. Lasave, F. Battaglini, R.D. Arce, R.R. Koropecki, Thin Solid Films 520 (2012) 6434.
[28] S. Libertino, V. Aiello, A. Scandurra, M. Renis, F. Sinatra, Sensors 8 (2008) 5637.
[29] S. Nakamura, S. Hayashi, K. Koga, Biochim. Biophys. Acta 445 (1976) 294.
[30] C. Xialing, M.J. Lin, Biochem. Technol. 1 (2009) 92.
[31] G. Raviola, Proc. Natl. Acad. Sci. U.S.A. 73 (1976) 638.
[32] M.H. Friedman, Principles and Models of Biological Transport, Springer, New York, 2008 (Chapter 2).
[33] P. Grathwohl, Diffusion in Natural Porous Media: Contaminant Transport, Sorption/Desorption and Dissolution Kinetics, Kluwer Academic Publishers, Boston, 1998.
[34] D.B. Hand, J. Biol. Chem. 108 (1934) 703.
[35] D.B. Hibbert, J.J. Gooding, P. Erokhin, Langmuir 18 (2002) 1770.
[36] W.H. Press, S.A. Teukolsky, W.T. Vetterling, B.P. Flannery, Numerical Recipes, Cambridge University Press, New York, USA, 1997.
[37] H. Ouyang, P.M. Fauchet, Proc. S.P.I.E.-Int. Soc. Opt. Eng. 6005 (2005) 6005081.
[38] D.A. Markov, K. Swinney, D.J. Bornhop, J. Am. Chem. Soc. 126 (2004) 16659.
[39] D.F. Dorfner, T. Hürlimann, T. Zabel, L.H. Frandsen, G. Abstreiter, J.J. Finley, Appl. Phys. Lett. 93 (2008) 181103.
[40] L.E. Valenti, P.A. Fiorito, C.D. García, C.E. Giacomelli, J. Colloid Interface Sci. 307 (2007) 349.
[41] R. Hérino, in: L. Canham (Ed.), Properties of Porous Silicon, INSPEC, London, 1997.
[42] S. Sun, P.H. Ho-Si, D.J. Harrison, Langmuir 7 (1991) 727.